



**HAL**  
open science

## Coral bleaching is linked to the capacity of the animal host to supply essential metals to the symbionts

Christine Ferrier-Pagès, Lucie Sauzéat, Vincent Balter

### ► To cite this version:

Christine Ferrier-Pagès, Lucie Sauzéat, Vincent Balter. Coral bleaching is linked to the capacity of the animal host to supply essential metals to the symbionts. *Global Change Biology*, 2018, 24 (7), pp.3145-3157. 10.1111/gcb.14141 . hal-03904891

**HAL Id: hal-03904891**

**<https://univ-lyon1.hal.science/hal-03904891>**

Submitted on 17 Dec 2022

**HAL** is a multi-disciplinary open access archive for the deposit and dissemination of scientific research documents, whether they are published or not. The documents may come from teaching and research institutions in France or abroad, or from public or private research centers.

L'archive ouverte pluridisciplinaire **HAL**, est destinée au dépôt et à la diffusion de documents scientifiques de niveau recherche, publiés ou non, émanant des établissements d'enseignement et de recherche français ou étrangers, des laboratoires publics ou privés.

***Coral bleaching is linked to the capacity of the animal host  
to supply essential metals to the symbionts***

***Running head: coral bleaching and metal availability***

**Christine Ferrier-Pagès<sup>1\*</sup>, Lucie Sauzéat<sup>2</sup>, Vincent Balter<sup>2</sup>**

1. Centre Scientifique de Monaco, 8 Quai Antoine 1er, MC-98000 Monaco, email:  
[ferrier@centrescientifique.mc](mailto:ferrier@centrescientifique.mc); tel: 00377 97774480

\* Corresponding author.

2. CNRS UMR 5276 "Laboratoire de Géologie de Lyon", Ecole Normale Supérieure de  
Lyon, 46, Allée d'Italie, 69364 Lyon Cedex 07, France.

Key words: coral bleaching; essential metals; heterotrophy; global warming; copper isotope;  
zinc isotope

Research article

25 **Abstract**

26 Massive coral bleaching events result in extensive coral loss throughout the world. These  
27 events are mainly caused by seawater warming, but are exacerbated by the subsequent  
28 decrease in nutrient availability in surface waters. It has therefore been shown that nitrogen,  
29 phosphorus, or iron limitation contribute to the underlying conditions by which thermal stress  
30 induces coral bleaching. Generally, information on the trophic ecology of metals in corals,  
31 and on how they modulate the coral response to thermal stress is lacking. Here, we  
32 demonstrate for the first time that heterotrophic feeding (*i.e.* the capture of zooplankton prey  
33 by the coral host) and thermal stress induce significant changes in the trace metal  
34 concentrations and isotopic signatures of the scleractinian coral *Stylophora pistillata*. The  
35 results obtained first reveal that coral symbionts are the major sink for the heterotrophically  
36 acquired metals and accumulate manganese, magnesium and iron from the food. These metals  
37 are involved in photosynthesis and anti-oxidant protection. In addition, we show that fed  
38 corals can maintain high metal concentrations in the host tissue during thermal stress and do  
39 not bleach, while unfed corals experience a significant decrease in copper, zinc, boron,  
40 calcium and magnesium in the host tissue and bleach. In addition, the significant increase in  
41  $\delta^{65}\text{Cu}$  and  $\delta^{66}\text{Zn}$  signature of symbionts and host tissue at high temperature suggests that these  
42 isotopic compositions are good proxy for stress in corals. Overall, present findings highlight a  
43 new way in which coral heterotrophy and metal availability contribute to coral resistance to  
44 global warming and bleaching.

45

## 46 **Introduction**

47 Mutualistic nutritional symbioses between animals and microorganisms are  
48 widespread in aquatic and terrestrial ecosystems, because they convey ecological advantages  
49 to the partners by allowing them to exploit a large panel of food sources (Douglas 1998; Saffo,  
50 1992; Venn, Loram, & Douglas, 2008). For example, cyanobacteria in symbiosis with lichens,  
51 or bacteria associated to insects, supply their host with essential amino acids (Douglas, 1998;  
52 Usher, Bergman, & Raven, 2007). Prominent and widely recognised nutritional symbioses in  
53 the marine environment are those formed between dinoflagellate algae and sea anemones,  
54 jellyfish, sponges, clams, or corals (Muscatine & Porter, 1977; Norton, Shepherd, Long, &  
55 Fitt, 1992). In particular, the association between corals and dinoflagellates of the genus  
56 *Symbiodinium* is at the basis of tropical reef ecosystems, which are as biodiverse as the rain  
57 forest, gathering more than 25% of all known marine species (Moberg & Folke 1999).

58 Dinoflagellates in symbiosis with corals transform inorganic into organic nutrients via  
59 photosynthesis and translocate most of their photosynthates to the animal host for its own  
60 nutritional needs (Muscatine, Falkowski, Porter, & Dubinsky, 1984; Tremblay, Grover,  
61 Maguer, Legendre, & Ferrier-Pagès, 2012). In turn, the host provides shelter to the  
62 dinoflagellates, but also nutrients from its metabolic waste products and/or its heterotrophic  
63 nutrition, i.e. the capture of zooplankton prey (Tremblay, Maguer, Grover, & Ferrier-Pagès,  
64 2015; Yellowlees, Rees, & Leggat, 2008). Since photosynthates cover almost 100% of the  
65 energetic needs of the symbiotic association in optimal living conditions, most studies until  
66 now have focused on better understanding the many services provided by dinoflagellates to  
67 corals under varying environmental conditions (reviewed in Davy, Allemand, & Weis, 2012;  
68 Tremblay, Grover, Maguer, Hoogenboom, & Ferrier-Pagès, 2014). The contrary, i.e., the  
69 amount and nature of heterotrophic nutrients translocated from the host to the symbionts have  
70 been very poorly studied (Hughes, Grottoli, Pease, & Matsui, 2010; Piniak, Lipschultz, &

71 McClelland, 2003; Tremblay, Maguer, Grover, & Ferrier-Pagès, 2015). Heterotrophy can  
72 however maintain the growth and metabolism of both symbionts and hosts whenever  
73 conditions are not favourable to autotrophy, such as in low-light environments (Anthony,  
74 2000), or during seawater warming, which leads to oxidative stress, symbiont expulsion  
75 (bleaching) and nutritional starvation (Ferrier-Pagès, Rottier, Beraud, & Levy, 2010; Grottoli,  
76 Rodrigues, & Palardy, 2006). The processes by which heterotrophy sustains coral metabolism  
77 during bleaching are not all known, except that particle capture is a major source of  
78 macronutrients (carbon, nitrogen and phosphorus), which enter into the composition of  
79 energetic reserves (Grottoli, Rodrigues, & Palardy, 2006; Hughes & Grottoli, 2013). In  
80 addition, heterotrophy promotes the re-establishment of photosynthate translocation after heat  
81 stress, suggesting that the symbionts are one of the main beneficiaries of this nutrient source  
82 (Tremblay, Gori, Maguer, Hoogenboom, & Ferrier-Pagès, 2016). Recently, genomic analyses  
83 also showed, in corals fed with zooplankton, an up-regulation of genes involved in the anti-  
84 oxidant response (Levy et al., 2016). Such response may be mediated through the  
85 heterotrophic supply of micronutrients (trace metals), which are constituents of anti-oxidant  
86 enzymes (Richier, Furla, Plantivaux, Merle, & Allemand, 2005), or which enter into the  
87 composition of photosynthetic pigments of the coral symbionts and are essential during  
88 bleaching (Shick et al., 2011).

89         Although the acquisition and allocation of autotrophic and heterotrophic  
90 macronutrients in corals start to be well studied via the use of stable isotope ratios such as  
91  $^{13}\text{C}/^{12}\text{C}$  and  $^{15}\text{N}/^{14}\text{N}$  (Hughes, Grottoli, Pease, & Matsui, 2010; Tremblay, Maguer, Grover, &  
92 Ferrier-Pagès, 2015), the trophic ecology of trace metals remains almost unknown, both under  
93 normal growth conditions and during thermal stress. To date, the wide majority of studies  
94 have focused on metal concentrations in coral skeletons to follow pollution events (Barnes,  
95 Taylor, & Lough, 1995; Bastidas & Garcia, 1999; David, 2003; Fallon, White, & McCulloch,

96 2002). Those performed at the tissue level showed that algal symbionts actively take up and  
97 accumulate trace metals dissolved in seawater (Ferrier-Pagès et al., 2005; Harland & Nganro,  
98 1990; Reichelt-Brushett & McOrist, 2003), suggesting that coral bleaching may result in  
99 metal limitation through symbiont loss. However, the changes in metal concentrations or  
100 isotopic signature of symbionts and host tissue with feeding and environmental stress are still  
101 unknown. As shown in other organisms such as mice and humans, isotopic signature of  
102 metals can be significantly affected by pathological conditions (e.g. Balter et al., 2015) as  
103 well as by dietary conditions (e.g. Jaouen, Pons, & Balter, 2013; Jaouen, Szpak, & Richards,  
104 2016, Costas-Rodríguez, Van Heghe, & Vanhaecke, 2014). This suggests that a change from  
105 autotrophic to heterotrophic feeding caused by bleaching conditions could also be marked by  
106 isotopic deregulations. In this study, we have investigated the trophic ecology of trace metals  
107 in the scleractinian coral *Stylophora pistillata* as well as the changes in the isotopic signature  
108 of copper and zinc under normal and thermal stress conditions. The first aim was to assess  
109 whether heterotrophy brings essential metals to the symbiotic association, and contributes, by  
110 this process, to increase the resistance of corals to thermal-stress induced bleaching. The  
111 second aim was to evaluate whether heterotrophy, and/or thermal stress, can be traced through  
112 a change in the isotopic signature of copper and zinc. Investigating those aspects allows for a  
113 better understanding of the processes leading to coral bleaching. The results will show  
114 whether bleaching is exacerbated by the lack of trace metals in coral tissue and whether  
115 zooplankton capture can supply these metals to corals.

116

## 117 **Materials and Methods**

### 118 Maintenance of coral colonies

119 Five colonies of the scleractinian coral *Stylophora pistillata* (Esper 1797), originating  
120 from the Red Sea (Aqaba, Jordan), were used to generate 40 large nubbins of ca. 10 cm long

121 (8 nubbins from each of the five colonies). Nubbins were then equally divided into 4  
122 treatments and two 20 L aquaria per treatment (8 aquaria in total). During the first five weeks,  
123 4 aquaria were fed during 2h and three times a week with 4000 *artemia salina* nauplii while  
124 the other 4 aquaria were kept unfed. All aquaria were maintained in an open flow system,  
125 with a water renewal rate of 10 L h<sup>-1</sup> and at a constant temperature of 25°C ± 0.5°C. Light was  
126 provided by hydrargyrum quartz iodide (HQI) lights at a photosynthetic active radiation level  
127 (PAR) of 200 μmol m<sup>-2</sup>s<sup>-1</sup> (measured using a spherical quantum sensor; LiCor LI-193,  
128 Lincoln, NE, USA), with a 12h:12h dark:light cycle. After these first 5 weeks, and for each  
129 feeding conditions, two aquaria were kept at 25°C while temperature was slowly raised (1°C  
130 every two days) in the two other aquaria to reach 30°C. Temperature and trophic conditions  
131 were maintained for three additional weeks prior measurements of trace metal concentrations  
132 and symbiont density were performed as described below.

133

#### 134 Treatments

135 Five nubbins in each condition were sampled for the determination of the symbiont  
136 density. Coral tissue was extracted from the skeleton using an air pick and homogenized with  
137 a Potter tissue grinder. The symbiont density was quantified with three sub-samples of 100 μL  
138 using a Z1 Coulter Particle Counter (Beckman Coulter). The five remaining nubbins in each  
139 condition were sampled, rinsed using artificial seawater (ASW) made with ultrapure sodium  
140 chloride (NaCl) (Trace Select for trace analysis ≥ 99.999%, Sigma Aldrich). They were then  
141 individually placed in 50 mL beakers (precombusted at 480°C for 4 h in a ThermolyneH  
142 62700 oven and rinsed with ASW) containing 5 mL of ASW. For each sample, tissue was  
143 completely removed from the skeleton with an air pick and homogenized with a Potter tissue  
144 grinder (treated as beakers). The homogenate was divided into a host and a symbiont fraction.  
145 For the host fraction, the homogenate was centrifuged (Biofuge 17RS Heraeus) at 3000 g for

146 10 min to pellet most of the symbionts. The supernatant was re-centrifuged twice to eliminate  
147 the remaining symbionts, then flash frozen with liquid nitrogen, and freeze-dried using a Heto  
148 (model CT 60) drier. For the symbiont fraction, the pellet was washed several times in ASW,  
149 flashed frozen and freeze-dried.

150

#### 151 Analyses of trace and major element concentrations

152 All chemical analyses were carried out in clean laminar flow hoods using double-  
153 distilled acids to avoid any exogenous contaminations. Freeze-dried coral and symbiont  
154 samples were dissolved in a concentrated HNO<sub>3</sub>-H<sub>2</sub>O<sub>2</sub> mixture, in Savillex beakers, at 120°C  
155 for at least 72h. Major and trace element concentrations were first measured in a small aliquot  
156 on an ICP-AES (iCAP 6000 Radial) and a quadrupole ICP-MS Thermo iCap-Q respectively  
157 at the Ecole Normale Supérieure (ENS) of Lyon following the method described in Garçon et  
158 al. (2017). Oxide interference and analytical drift were corrected using indium (In) and  
159 scandium (Sc) addition as internal standards for trace and major elements respectively (Sigma  
160 Aldrich, France). In-house (sheep plasma, OEP) and international standards (bovine liver,  
161 1577c, Sigma Aldrich) as well as complete duplicate and re-run analyses were measured to  
162 ensure the validity and assess the precision of our results. Metal concentrations are all  
163 reported in µg g<sup>-1</sup> (ppm) dry weight.

164

#### 165 Analyses of copper and zinc isotopic compositions

166 Copper and zinc isotopic compositions were then measured following the procedure  
167 described by Maréchal, Télouk, & Albarède, (1999). Briefly, before each isotopic  
168 measurement, samples were purified by ion-exchange chromatography using quartz columns  
169 filled with 1.8 mL of Bio-Rad AGMP-1 (100-200 mesh) anion-exchange resin. Copper was  
170 first eluted with 20 mL of HCl (7 mol L<sup>-1</sup>) + 0.001% H<sub>2</sub>O<sub>2</sub> followed by zinc with 10 mL of



171 HNO<sub>3</sub> (0.5 mol L<sup>-1</sup>). The purification step helps removing elements (e.g. Ni, Ti, Al or Ba),  
172 which may interfere with copper and zinc during the instrumental measurement (Chen et al.,  
173 2016; Sossi, Halverson, Nebel, & Eggins, 2014). Indeed, it has been shown that small  
174 amounts of Ni and Ti residues, for example, can produce isobaric interferences and shift the  
175 measured δ<sup>66</sup>Zn values by more than 0.07 ‰ if the Ni/Zn and Ti/Zn ratios are higher than  
176 0.001 and 0.01, respectively (Chen et al., 2016).

177 On the day of the analyses, an aliquot of the Zn and Cu purified solutions, previously  
178 evaporated to dryness, are dissolved in a Cu (Cu SRM 976, National Institute of Standards  
179 and Technology, Gaithersburg, MD, USA) or Zn-doped solution (Zn JMC 3-0749L, Johnson  
180 Matthey Royston, UK) respectively to reach sample concentration of about 300 µg L<sup>-1</sup> that is  
181 similar to the concentration of the standard solution that was run between each sample. Both  
182 copper and zinc isotopic compositions, expressed as

$$183 \quad \delta^{65}\text{Cu}_{\text{sample}} (\text{in } \text{‰}) = \left[ \frac{\left( \frac{{}^{65}\text{Cu}}{{}^{63}\text{Cu}} \right)_{\text{sample}}}{\left( \frac{{}^{65}\text{Cu}}{{}^{63}\text{Cu}} \right)_{\text{standard}}} - 1 \right] * 1000$$

$$184 \quad \delta^{66}\text{Zn}_{\text{sample}} (\text{in } \text{‰}) = \left[ \frac{\left( \frac{{}^{66}\text{Zn}}{{}^{64}\text{Zn}} \right)_{\text{sample}}}{\left( \frac{{}^{66}\text{Zn}}{{}^{64}\text{Zn}} \right)_{\text{standard}}} - 1 \right] * 1000$$

185 were measured on a Nu Plasma (Nu 500) MC-ICP-MS in wet plasma conditions. Instrumental  
186 mass fractionation was corrected with an exponential law using an elemental-doping method  
187 as recommended by Maréchal, Télouk, & Albarède, (1999). δ<sup>66</sup>Zn and δ<sup>65</sup>Cu were then  
188 calculated by standard bracketing using Zn JMC 3-0749L (Johnson Matthey Royston, UK)  
189 and Cu SRM 976 (NIST, Gaithersburg, MD, USA) as reference standards. Note that these  
190 standards were repeatedly measured between each sample to correct for the instrumental drift  
191 throughout the analytical sequence; a method called standard bracketing. The accuracy of the  
192 isotopic compositions was assessed based on the analyses of an in-house (sheep plasma; OEP)  
193 and international (bovine liver, 1577c, Sigma Aldrich, France) standard solution at the

194 beginning and during the analytical sequence. The average  $\delta^{66}\text{Zn}$  measured for the in-house  
195 standard solution was  $+0.75\text{ ‰} \pm 0.07$  and  $-1.19\text{ ‰} \pm 0.07$  for  $\delta^{65}\text{Cu}$  which is in good  
196 agreement with our previous reference in-house values ( $\delta^{65}\text{Cu} = -1.15\text{ ‰} \pm 0.20$  (standard  
197 deviation (sd),  $n = 35$ ) and  $\delta^{66}\text{Zn} = +0.73\text{ ‰} \pm 0.09$  (sd,  $n = 20$ ). Our results for the  
198 international standard (1577c) are also in good agreements with previous results:  $\delta^{66}\text{Zn}_{\text{this study}}$   
199  $= -0.20\text{ ‰} \pm 0.06$  (sd,  $n = 10$ ) compared to  $\delta^{66}\text{Zn}_{1577c} = -0.16\text{ ‰} \pm 0.15$  (sd,  $n = 45$ ) and  
200  $\delta^{65}\text{Cu}_{\text{this study}} = +0.30\text{ ‰} \pm 0.13$  (sd,  $n = 10$ ) compared to  $\delta^{65}\text{Cu}_{1577c} = +0.37\text{ ‰} \pm 0.14$  (sd,  $n =$   
201  $43$ ). Based on re-run samples and complete duplicate analyses, we estimate the precision of  
202 our measurements at  $\pm 0.1$  (sd) for both  $\delta^{65}\text{Cu}$  and  $\delta^{66}\text{Zn}$ . The long-term precision based on  
203 the repeated measurements of standard Zn JMC 3-0749L and Cu SRM 976 alone is similar ( $\pm$   
204  $0.07\text{ ‰}$  (sd,  $n = 480$ )).

205

## 206 Statistics

207 A correlation-based principal component analysis (PCA) was used to quantify the effect of  
208 thermal stress and heterotrophic feeding on the chemical composition of symbionts and host  
209 tissue of colonies of *Sylophora pistillata*. The method consists in identifying new variables  
210 called principal components (PCs), which are linear combination of the original variables and  
211 along which data variation is maximal. For each principal component (PC), linear regressions,  
212 using standard least-squares techniques, were thus used to estimate the relationship between  
213 parameters. In this study, the variables include the chemical concentrations of the trace  
214 elements measured in host tissue and symbionts (manganese, iron, magnesium, zinc,  
215 strontium, arsenic, barium, calcium, boron and copper), as well as copper ( $\delta^{65}\text{Cu}$ ) and zinc  
216 ( $\delta^{66}\text{Zn}$ ) isotopic compositions. All data were log transformed and normalized, and samples  
217 with incomplete data were excluded. PCA was implemented in MATLAB™.

218 Statistical analyses: all parameters were expressed as mean  $\pm$  standard deviation (SD) of five

219 measurements. Statistical analyses were performed using Systat 13 software (Systat Software,  
220 Chicago, IL, USA). Data were checked for normality using the Kolmogorov-Smirnov test  
221 with Lilliefors correction and for homoscedasticity using Levene test. Data were transformed  
222 with a natural logarithm transformation when required (i.e. Fe, Sr, Ca and B in symbionts; Fe,  
223 Mg, Zn, Ba, Ca and B in coral host). Factorial ANOVA with two factors (feeding an  
224 temperature) were performed and when there were significant differences between treatments,  
225 analyses were followed by a posteriori testing (Tukey's test). Differences between factors  
226 were considered significant for p-values < 0.05.

227

## 228 **Results**

229 The PCA yielded two principal components (PC1 and PC2) that explain ca. 70% of  
230 the total variance (Fig. 1). In this figure, grey arrows graphically represent the loading factors  
231 (i.e. weight of each variable on PC1 and PC2, and Table S1). The first component (PC1),  
232 which explains 44% of the total variance, is defined by positive correlations with several trace  
233 elements such as iron (Fe), barium (Ba) or boron (B). This principal component demonstrates  
234 that symbionts contained higher metal concentrations ( $\mu\text{g g}^{-1}$  dry weight) than the animal  
235 tissue, suggesting that metals were not distributed equally in these two compartments.  
236 Principal component 2 (PC2) explains 25% of the total variance and is defined by relatively  
237 high weights from Cu, but negative correlation with magnesium (Mg),  $\delta^{65}\text{Cu}$  and  $\delta^{66}\text{Zn}$ . This  
238 principal component separates both symbionts and animal tissues maintained at 25°C and  
239 30°C, showing that thermal stress was associated with variation in both their metal content  
240 and isotopic composition. As demonstrated by the PCA and the results summarised in Table 1,  
241 for both temperatures investigated (25°C and 30°C), and in all feeding conditions, symbionts  
242 presented higher metal concentrations ( $\mu\text{g g}^{-1}$  dry weight) than the animal tissue, except for  
243 Mg, whose concentration tended to be slightly higher in the host tissue (Fig.1).

244 The two factors ANOVA (Table 2) shows significant effect of both feeding and  
245 temperature, alone or in combination, on the micronutrient concentrations of symbionts and  
246 animal tissue. At the normal growth temperature (25°C), symbionts of fed colonies presented  
247 higher concentrations of Mg (post-hoc, p-value= 0.002), Fe (p-value= 0.003) and Mn, (p-  
248 value <0.001), but lower concentrations of strontium (Sr), and arsenic (As) (p-value= 0.01  
249 and 0.004 respectively) than symbionts of unfed colonies (Table S2). Inversely, there was no  
250 significant difference in trace metal concentrations between fed and unfed coral tissue at 25°C  
251 (Table S3, post-hoc, p value >0.1). Host tissue of fed corals had however a higher  $\delta^{65}\text{Cu}$   
252 signature ( $-0.42\text{‰} \pm 0.12$ , ANOVA, p value = 0.0455) than the host tissue of unfed corals ( $-$   
253  $0.67\text{‰} \pm 0.05$  respectively) (Fig. 2).

254 Thermal stress (30°C) induced a significant bleaching in unfed colonies (t-test, p-value  
255 = 0.0016), with a 50% reduction in symbiont density (Fig. 2). On the contrary, it had no effect  
256 on the symbiont density of fed colonies, which also presented two times more symbionts (Fig.  
257 2). Thermal stress significantly changed the metal concentrations (Tables 1, 2 and Tables S2,  
258 S3) of the symbiotic association. There was a significant increase of Sr, Ca, Zn and B  
259 concentrations in both symbionts and host of fed and unfed colonies (Tables 1 and 2). High  
260 temperature also significantly increased Mg concentrations in fed host tissue and unfed  
261 symbionts, Ba in fed and unfed symbionts, as well as Mn in the host tissue of fed corals  
262 (Tables 2, S2, S3). On the contrary, the Cu content of fed and unfed colonies was  
263 significantly decreased (Table 2). Finally, thermal stress significantly increased the  $\delta^{65}\text{Cu}$  and  
264  $\delta^{66}\text{Zn}$  values of both host and symbionts, independently of the feeding status (Fig. 2).

265 The binary plot of Fig. 3a shows that there was an overall increase in both the  $\delta^{65}\text{Cu}$   
266 and  $\delta^{66}\text{Zn}$  values with thermal stress in corals and symbionts. The other binary plots  
267 performed with metal concentrations (Fig. 3b to 3f) exhibit two thermal stress patterns on fed  
268 and unfed coral colonies: data corresponding to fed and unfed host or fed and unfed

269 symbionts are tightly clustered at 25°C, suggesting that at this temperature there is no effect  
270 of the dietary regime. The same pattern is observed for all symbionts at 30°C, suggesting that  
271 they obtain the same amount of metals from their respective fed and unfed hosts. On the  
272 contrary, metal concentrations in the host show a distillation process at 30°C, associated to a  
273 metal depletion in unfed hosts compared to fed ones (red arrows bleaching, Fig. 3b to f). The  
274 amplitude by which hosts are depleted increases as the metal concentrations decrease.

275

## 276 **Discussion**

277         Understanding the nutritional requirements of scleractinian corals is critical to assess  
278 their health status and predict how reefs will change in response to rising seawater  
279 temperatures (Connolly, Lopez-Yglesias, & Anthony, 2012; Ferrier-Pagès, Rottier, Beraud, &  
280 Levy, 2010). The main finding of this study is that heterotrophic feeding brings essential  
281 metals to corals, which are mainly accumulated in the symbionts, and help avoid thermal  
282 stress damages and subsequent bleaching. During thermal stress, symbionts retain metals at  
283 the expense of the coral host, thus being more parasites than symbionts. We also demonstrate  
284 a significant disruption in the Ca, Mg, Sr and B homeostasis in coral tissue during thermal  
285 stress, as well as a significant increase in the  $\delta^{65}\text{Cu}$  and  $\delta^{66}\text{Zn}$  values of coral host and  
286 symbionts. These isotopic compositions thus constitute good proxies for thermal stress in  
287 corals.

288

### 289 **1- Effect of the dietary regime at 25°C**

290         Symbionts were the main sink for micronutrients within the symbiotic association  
291 (Fig. 1), although these nutrients were provided to corals as particulate organic food, first  
292 digested by the animal. This observation is contrary to the usual view that symbionts are the  
293 main food suppliers of the symbiotic association, and provides one of the rare evidence of

294 inverse nutrient translocation, from the animal host to the symbionts (Piniak, Lipschultz, &  
295 McClelland, 2003; Tremblay, Maguer, Grover, & Ferrier-Pagès 2015). Although the above  
296 studies showed that symbionts profited from heterotrophic macronutrients (carbon, nitrogen)  
297 entering the symbiotic association, the transfer was restricted to less than 20% of the total  
298 gain, against 100% in this study.

299 Plankton feeding significantly increased, in symbiont cells, the concentrations of three  
300 main micronutrients, namely Mn, Fe and Mg (Table 1). Among other functions, Mn, Fe and  
301 Mg are all involved in the composition of anti-oxidant enzymes (Krueger et al., 2015). These  
302 enzymes, such as catalases, peroxidases and Fe/Mn or Mn-superoxide dismutases (SOD), are  
303 present in *Symbiodinium* (Lin et al., 2015; Zhang, Zhuang, Gill, & Lin, 2013), and are used to  
304 scavenge reactive oxygen species (ROS) continuously produced through photosynthesis and  
305 over-produced during thermal stress (Weis, 2008). Mn and Fe also play a major role in  
306 photosynthesis, nitrate reduction, as well as in chlorophyll and amino acid synthesis (Twining  
307 & Baines, 2013). This involvement of Fe and Mn in photosynthetic processes is one of the  
308 explanations why symbiont density, chlorophyll content, and photosynthetic rates are  
309 significantly enhanced in heterotrophically-fed coral colonies compared to unfed ones, both in  
310 normal growth and stress conditions (this study and reviewed in Houlbrèque & Ferrier-Pagès,  
311 2009). On the contrary, a lack of Fe during thermal stress increases the bleaching  
312 susceptibility of corals (Shick et al., 2011). Overall, these results highlight the importance of  
313 Fe and other key micronutrient availability for coral photosynthesis and health. Whereas  
314 concentrations of Fe, Mn, Mg were enhanced in fed symbionts under normal growth  
315 conditions, concentrations of Ca and Sr, which are main components of coral skeletons, were  
316 significantly decreased (Table 1). Such changes may be linked to a higher translocation of  
317 these elements to the skeleton, since fed corals present higher calcification rates than unfed  
318 corals (Houlbrèque & Ferrier-Pagès, 2009). The schematic diagram of Fig. 4 summarizes the

319 findings observed in this study and the potential role of metals in symbionts, under normal  
320 growth conditions of *S. pistillata*.

321

322 The  $\delta^{65}\text{Cu}$  and  $\delta^{66}\text{Zn}$  values were significantly different between fed and unfed hosts  
323 and symbionts (Fig. 2), suggesting, for the first time, that corals fractionate Cu and Zn  
324 isotopes depending on their dietary regime. The higher  $\delta^{65}\text{Cu}$  values in fed colonies is linked  
325 to the consumption of Cu in the form of particulate organic matter, while unfed colonies only  
326 rely on the uptake of dissolved inorganic Cu by the symbionts. The  $\delta^{65}\text{Cu}$  signature in fed  
327 corals indeed follows the rule that organic matter is enriched in the heavier Cu isotope  
328 compared to dissolved inorganic Cu (Petit et al., 2013). The lower  $\delta^{66}\text{Zn}$  signature of fed  
329 compared to unfed colonies is also in agreement with the observation that carnivores are  
330 slightly  $^{66}\text{Zn}$ -depleted relative to herbivores (Jaouen, Szpak, & Richards, 2016). Overall, the  
331 significant effect of feeding on the  $\delta^{66}\text{Zn}$  and  $\delta^{65}\text{Cu}$  signatures demonstrates that metal  
332 isotopes represent useful proxies to trace nutrient flows within a symbiotic association,  
333 although they have poorly been studied in marine food webs in general (Jaouen, Szpak, &  
334 Richards, 2016).

335

## 336 **2- Effect of thermal stress**

337 After three weeks of thermal stress, which induced bleaching in unfed corals (Fig. 2),  
338 significant changes occurred in metal concentrations and Cu-Zn isotopic compositions of  
339 symbionts and host tissue under both fed and unfed conditions. We observed a clear increase  
340 in the  $\delta^{65}\text{Cu}$  and  $\delta^{66}\text{Zn}$  values of both hosts and symbionts (Fig. 3A). Such isotopic variations  
341 can be related to an increase in reactive oxygen species (ROS) generated by thermal stress in  
342 coral tissue (Cunning & Baker, 2013). As light isotopes create weaker links with molecules  
343 compared to heavy isotopes (Schauble, 2004), these bonds are more easily disrupted by ROS

344 (Demidov, 2007; Shepinov & Pestov, 2010). Light isotopes will thus preferentially be  
345 released in the medium. Although this assumption still needs to be verified, we can already  
346 suggest that  $\delta^{65}\text{Cu}$  and  $\delta^{66}\text{Zn}$  signatures represent good proxies for thermal stress in corals. In  
347 addition, the correlation which existed between  $\delta^{65}\text{Cu}$  and  $\delta^{66}\text{Zn}$  at 25°C was lost at 30°C  
348 (Fig. 3), suggesting that animals and symbionts were not in equilibrium any more at 30°C.

349 For all corals, thermal stress also induced a very large increase of the Mg, Sr, Ca and  
350 B concentrations compared to normal growth conditions, in particular in symbionts of unfed  
351 colonies. Although such changes have never been investigated in corals, an increase in  
352 intracellular Ca concentration has been monitored in insects (Teets, Yi, Lee, & Denlinger,  
353 2013), chicken lymphocytes (Han et al., 2010) or terrestrial plants (Zhu, 2001) during thermal  
354 stress, while an increase in Mg was observed in the shrimp *Crangon crangon* (Sartoris &  
355 Pörtner, 1997). Genomic studies, which have investigated the molecular basis of cnidarian  
356 bleaching, also suggested that Ca homeostasis was disrupted in heat-stressed corals (DeSalvo  
357 et al., 2008; Levy et al., 2016; Rodriguez-Lanetty, Harii, & Hoegh-Guldberg, 2009). Finally,  
358 Dishon et al., (2015) demonstrated a decline of  $\delta^{11}\text{B}$  as a result of coral bleaching, likely due,  
359 according to our results, to the observed large increase in B concentration, which should have  
360 changed the intracellular pH. All these metals play important cellular roles. Ca is an  
361 intracellular messenger, while Mg has a protective role against oxidative damage (Freedman  
362 et al., 1992; Sartoris & Pörtner, 1997), which suggests that the significant Mg increase in  
363 coral cells followed the temperature-induced ROS production (Weis, 2008). Finally, B is  
364 needed, among others, for membrane structural integrity and carbohydrate metabolism  
365 (reviewed in Pilbeam & Kirkby, 1983), two important processes in corals.

366 Despite the large internal changes induced by thermal stress, mixotrophic corals (fed  
367 with artemia) did not bleach while autotrophic corals did. The lack of bleaching, as well as the  
368 maintenance of high rates of photosynthesis and calcification in mixotrophic corals have been



369 observed several times in previous studies (Borell & Bishof, 2008; Connolly, Lopez-Yglesias,  
370 & Anthony, 2012; Ferrier-Pagès, Rottier, Beraud, & Levy, 2010). The binary plots of metal  
371 concentrations in fed and unfed coral colonies (Fig. 3B to 3F) highlight a new mechanism by  
372 which heterotrophy sustains coral metabolism during thermal stress, e.g. via the supply of  
373 essential metals to the host and symbionts. These plots show similar metal concentrations in  
374 symbionts of both fed and unfed colonies during thermal stress. In other words, symbionts  
375 sequestered the same amount of metals irrespective of the feeding status of their host. As  
376 metals are mostly translocated from the host to the symbionts, this led to two different metal  
377 conditions in host tissue depending on the feeding status of the colonies. In fed corals,  
378 heterotrophy supplied enough metals to the host to sustain symbiont's needs and no bleaching  
379 is observed. In unfed corals, symbiont repletion lead to a significant depletion of metals in  
380 host tissue (Fig. 3B to F), and a cost for the symbiotic association, which underwent  
381 bleaching and nutrient starvation. The amplitude by which hosts were depleted increased as  
382 the metal concentrations decreased. These results thus demonstrate the significant effect of  
383 feeding in providing metals to the animals during thermal stress. The significant bleaching in  
384 unfed colonies further suggests that, contrary to fed corals, metal concentrations in unfed host  
385 tissue were not sufficient to sustain high densities of symbionts. Finally, they also suggest that  
386 thermal stress has promoted symbiont parasitism in unfed corals. A similar selfish behaviour  
387 of symbionts during thermal stress has very recently been observed for macronutrients (Baker  
388 et al. 2018). Figure 5 summarizes the findings and hypotheses on the role of metals in coral  
389 bleaching.

390 In summary, our results indicate that the  $\delta^{65}\text{Cu}$  and  $\delta^{66}\text{Zn}$  values represent good  
391 proxies for stress in corals. They also show that heterotrophy and thermal stress induce  
392 significant changes in trace metal concentrations and isotopic signatures of the scleractinian  
393 coral *Stylophora pistillata*. The results obtained first reveal that symbionts are the major sink

394 for trace metals in the symbiotic association, and accumulate Mn, Mg and Fe from the  
395 heterotrophic feeding of the host. They also demonstrate that bleaching is exacerbated by the  
396 shortage of trace metals in coral tissue (especially Cu, Zn, B, Mg, Ca) and that heterotrophic  
397 feeding can supply these essential metals to corals. Such results thus highlight a new way by  
398 which heterotrophy contributes to coral resistance to bleaching, and have major implications  
399 for the resilience of coral reefs under threat of global change.

400

#### 401 **Acknowledgements**

402 The authors would like to thank Cecile Rottier and Magali Boussion for help in coral  
403 extraction. We also thank two reviewers, and Prof. Oren Levy, for their helpful comments,  
404 which have greatly improved the manuscript. This work is part of RTPI Nutress (Réseau  
405 Thématique Pluridisciplinaire International sur l'Ecophysiologie de la Nutrition).

406

#### 407 **References**

- 408 Anthony, K. R. N. (2000). Enhanced particle-feeding capacity of corals on turbid reefs (Great  
409 Barrier Reef, Australia). *Coral reefs*, 19(1), 59-67.
- 410 Balter, V., da Costa, A. N., Bondanese, V. P., Jaouen, K., Lamboux, A., Sangrajrang, S.,  
411 Vincent, N., Fourel, F., Telouk, P., Gigou, M., Lécuyer, C., Srivatanakul, P., Bréchet, C.,  
412 Albarède, F., & Heynaud, P. (2015). Natural variations of copper and sulfur stable isotopes  
413 in blood of hepatocellular carcinoma patients. *Proceedings of the National Academy of*  
414 *Sciences*, 112(4), 982-985.
- 415 Barnes, D. J., Taylor, R. B., & Lough, J. M. (1995). On the inclusion of trace materials into  
416 massive coral skeletons. Part II: distortions in skeletal records of annual climate cycles due  
417 to growth processes. *Journal of Experimental Marine Biology and Ecology*, 194(2), 251-  
418 275.

419 Bastidas, C., & García, E. (1999). Metal content on the reef coral *Porites astreoides*: an  
420 evaluation of river influence and 35 years of chronology. *Marine Pollution Bulletin*,  
421 38(10), 899-907.

422 Borell, E. M., & Bischof, K. (2008). Feeding sustains photosynthetic quantum yield of a  
423 scleractinian coral during thermal stress. *Oecologia*, 157(4), 593.

424 Chen, S., Liu, Y., Hu, J., Zhang, Z., Hou, Z., Huang, F., & Yu, H. (2016). Zinc Isotopic  
425 Compositions of NIST SRM 683 and Whole-Rock Reference Materials. *Geostandards and*  
426 *Geoanalytical Research*, 40(3), 417-432.

427 Connolly, S. R., Lopez-Yglesias, M. A., & Anthony, K. R. (2012). Food availability promotes  
428 rapid recovery from thermal stress in a scleractinian coral. *Coral reefs*, 31(4), 951-960.

429 Costas-Rodríguez, M., Van Heghe, L., & Vanhaecke, F. (2014). Evidence for a possible  
430 dietary effect on the isotopic composition of Zn in blood via isotopic analysis of food  
431 products by multi-collector ICP-mass spectrometry. *Metallomics*, 6, 139–146.

432 Cunning, R., & Baker, A. C. (2013). Excess algal symbionts increase the susceptibility of reef  
433 corals to bleaching. *Nature Climate Change*, 3(3), 259-262.

434 David, C. P. (2003). Heavy metal concentrations in growth bands of corals: a record of mine  
435 tailings input through time (Marinduque Island, Philippines). *Marine Pollution Bulletin*,  
436 46(2), 187-196.

437 Davy, S. K., Allemand, D., & Weis, V. M. (2012). Cell biology of cnidarian-dinoflagellate  
438 symbiosis. *Microbiology and Molecular Biology Reviews*, 76(2), 229-261.

439 Demidov, V. V. (2007). Heavy isotopes to avert ageing? *Trends in biotechnology*, 25(9), 371-  
440 375.

441 DeSalvo, M. K., Voolstra, C. R., Sunagawa, S., Schwarz, J. A., Stillman, J. H., Coffroth, M.  
442 A., Szmant A. M., & Medina, M. (2008). Differential gene expression during thermal

443 stress and bleaching in the Caribbean coral *Montastraea faveolata*. *Molecular ecology*,  
444 17(17), 3952-3971.

445 Dishon, G., Fisch, J., Horn, I., Kaczmarek, K., Bijma, J., Gruber, D. F., Nir, O., Popovich, Y.,  
446 & Tchernov, D. (2015). A novel paleo-bleaching proxy using boron isotopes and high-  
447 resolution laser ablation to reconstruct coral bleaching events. *Biogeosciences*, 12(19),  
448 5677-5687.

449 Douglas, A. E. (1998). Nutritional interactions in insect-microbial symbioses: aphids and their  
450 symbiotic bacteria Buchnera. *Annual review of entomology*, 43(1), 17-37.

451 Fallon, S. J., White, J. C., & McCulloch, M. T. (2002). Porites corals as recorders of mining  
452 and environmental impacts: Misima Island, Papua New Guinea. *Geochimica et*  
453 *Cosmochimica Acta*, 66(1), 45-62.

454 Ferrier-Pagès, C., Houlbrèque, F., Wyse, E., Richard, C., Allemand, D., & Boisson, F. (2005).  
455 Bioaccumulation of zinc in the scleractinian coral *Stylophora pistillata*. *Coral Reefs*, 24(4),  
456 636-645.

457 Ferrier-Pagès, C., Rottier, C., Beraud, E., & Levy, O. (2010). Experimental assessment of the  
458 feeding effort of three scleractinian coral species during a thermal stress: Effect on the  
459 rates of photosynthesis. *Journal of Experimental Marine Biology and Ecology*, 390(2),  
460 118-124.

461 Freedman, A. M., Mak, I. T., Stafford, R. E., Dickens, B. F., Cassidy, M. M., Muesing, R. A.,  
462 & Weglicki, W. B. (1992). Erythrocytes from magnesium-deficient hamsters display an  
463 enhanced susceptibility to oxidative stress. *American Journal of Physiology*, 262:C1371–  
464 C1375.

465 Garçon, M., Sauzéat, L., Carlson, R. W., Shirey, S. B., Simon, M., Balter, V., & Boyet, M.  
466 (2017). Nitrile, Latex, Neoprene and Vinyl Gloves: A Primary Source of Contamination

467 for Trace Element and Zn Isotopic Analyses in Geological and Biological Samples.  
468 *Geostandards and Geoanalytical Research*.

469 Grottoli, A. G., Rodrigues, L. J., & Palardy, J. E. (2006). Heterotrophic plasticity and  
470 resilience in bleached corals. *Nature*, 440(7088), 1186-1189.

471 Han, A. Y., Zhang, M. H., Zuo, X. L., Zheng, S. S., Zhao, C. F., Feng, J. H., & Cheng, C.  
472 (2010). Effect of acute heat stress on calcium concentration, proliferation, cell cycle, and  
473 interleukin-2 production in splenic lymphocytes from broiler chickens. *Poultry science*,  
474 89(10), 2063-2070.

475 Harland, A. D., & Nganro, N. R. (1990). Copper uptake by the sea anemone *Anemonia viridis*  
476 and the role of zooxanthellae in metal regulation. *Marine Biology*, 104(2), 297-301.

477 Houlbrèque, F., & Ferrier-Pagès, C. (2009). Heterotrophy in tropical scleractinian corals.  
478 *Biological Reviews*, 84(1), 1-17.

479 Hughes, A. D., & Grottoli, A. G. (2013). Heterotrophic compensation: a possible mechanism  
480 for resilience of coral reefs to global warming or a sign of prolonged stress? *PLoS One*,  
481 8(11), e81172.

482 Hughes, A. D., Grottoli, A. G., Pease, T. K., & Matsui, Y. (2010). Acquisition and  
483 assimilation of carbon in non-bleached and bleached corals. *Marine Ecology Progress*  
484 *Series*, 420, 91-101.

485 Jaouen, K., Pons, M., L., & Balter, V. (2013) Iron, copper and zinc isotopic fractionation up  
486 mammal trophic chains. *Earth and Planetary Science Letters*, 374, 164-172.

487 Jaouen, K., Szpak, P., & Richards, M. P. (2016). Zinc isotope ratios as indicators of diet and  
488 trophic level in arctic marine mammals. *PloS one*, 11(3), e0152299.

489 Krueger, T., Fisher, P. L., Becker, S., Pontasch, S., Dove, S., Hoegh-Guldberg, O., Leggat,  
490 W., & Davy, S. K. (2015). Transcriptomic characterization of the enzymatic antioxidants

491 FeSOD, MnSOD, APX and KatG in the dinoflagellate genus *Symbiodinium*. *BMC*  
492 *evolutionary biology*, 15(1), 48.

493 Levy, O., Karako-Lampert, S., Ben-Asher, H. W., Zoccola, D., Pagès, G., & Ferrier-Pagès, C.  
494 (2016). Molecular assessment of the effect of light and heterotrophy in the scleractinian  
495 coral *Stylophora pistillata*. *Proceedings Royal Society B*, 283, 20153025.

496 Lin, S., Cheng, S., Song, B., Zhong, X., Lin, X., Li, W., et al. (2015). The *Symbiodinium*  
497 Kawaguti genome illuminates dinoflagellate gene expression and coral symbiosis. *Science*,  
498 350, 691-694.

499 Maréchal, C. N., Télouk, P., & Albarède, F. (1999). Precise analysis of copper and zinc  
500 isotopic compositions by plasma-source mass spectrometry. *Chemical Geology*, 156(1),  
501 251-273.

502 Miller, K.A., Keenan, C.M., Martin, G.R., Jirik, F.R., Sharkey, K.A., & Wieser, M.E. (2016).  
503 The expression levels of cellular prion protein affect copper isotopic shifts in the organs of  
504 mice. *Journal of Analytical Atomic Spectrometry*, 31, 2015-2022 .

505 Moberg, F., & Folke, C. (1999). Ecological goods and services of coral reef ecosystems.  
506 *Ecological economics*, 29(2), 215-233.

507 Muscatine, L., Falkowski, P. G., Porter, J. W., & Dubinsky, Z. (1984). Fate of photosynthetic  
508 fixed carbon in light-and shade-adapted colonies of the symbiotic coral *Stylophora*  
509 *pistillata*. *Proceedings of the Royal Society of London B: Biological Sciences*, 222(1227),  
510 181-202.

511 Muscatine, L., & Porter, J. W. (1977). Reef corals: mutualistic symbioses adapted to nutrient-  
512 poor environments. *Bioscience*, 27(7), 454-460.

513 Norton, J. H., Shepherd, M. A., Long, H. M., & Fitt, W. K. (1992). The zooxanthellal tubular  
514 system in the giant clam. *The Biological Bulletin*, 183(3), 503-506.

515 Petit, J. C., Schäfer, J., Coynel, A., Blanc, G., Deycard, V. N., Derriennic, H., Lancelleur, L.,  
516 Dutruch L., Bossy C., & Mattielli, N. (2013). Anthropogenic sources and biogeochemical  
517 reactivity of particulate and dissolved Cu isotopes in the turbidity gradient of the Garonne  
518 River (France). *Chemical Geology*, 359, 125-135.

519 Pilbeam, D. J., & Kirkby, E. A. (1983). The physiological role of boron in plants. *Journal of*  
520 *Plant Nutrition*, 6(7), 563-582.

521 Piniak, G. A., Lipschultz, F., & McClelland, J. (2003). Assimilation and partitioning of prey  
522 nitrogen within two anthozoans and their endosymbiotic zooxanthellae. *Marine Ecology*  
523 *Progress Series*, 262, 125-136.

524 Reichelt-Brushett, A. J., & McOrist, G. (2003). Trace metals in the living and nonliving  
525 components of scleractinian corals. *Marine Pollution Bulletin*, 46(12), 1573-1582.

526 Richier, S., Furla, P., Plantivaux, A., Merle, P. L., & Allemand, D. (2005). Symbiosis-induced  
527 adaptation to oxidative stress. *Journal of Experimental Biology*, 208(2), 277-285.

528 Rodriguez-Lanetty, M., Harii, S., & Hoegh-Guldberg, O. (2009). Early molecular responses  
529 of coral larvae to hyperthermal stress. *Molecular ecology*, 18(24), 5101-5114.

530 Saffo, M. B. (1992). Coming to terms with a field: words and concepts in symbiosis.  
531 *Symbiosis*, 14(1-3), 17-31.

532 Sartoris, F. J., & Pörtner, H. O. (1997) Increased concentrations of haemolymph Mg<sup>2+</sup>  
533 protect intracellular pH and ATP levels during temperature stress and anoxia in the  
534 common shrimp. *Journal of Experimental Biology*, 200, 785-792.

535 Schauble, E. A. (2004). Applying stable isotope fractionation theory to new systems. *Reviews*  
536 *in Mineralogy and Geochemistry*, 55(1), 65-111.

537 Shick, J. M., Iglie, K., Wells, M. L., Trick, C. G., Doyle, J., & Dunlap, W. C. (2011).  
538 Responses to iron limitation in two colonies of *Stylophora pistillata* exposed to high

539 temperature: Implications for coral bleaching. *Limnology and Oceanography*, 56(3), 813-  
540 828.

541 Sossi, P. A., Halverson, G. P., Nebel, O., & Eggins, S. M. (2014). Combined separation of  
542 Cu, Fe and Zn from rock matrices and improved analytical protocols for stable isotope  
543 determination. *Geostandards and Geoanalytical Research*, 39(2), 129-149.

544 Teets, N. M., Yi, S. X., Lee, R. E., & Denlinger, D. L. (2013). Calcium signaling mediates  
545 cold sensing in insect tissues. *Proceedings of the National Academy of Sciences*, 110(22),  
546 9154-9159.

547 Tremblay, P., Maguer, J. F., Grover, R., & Ferrier-Pagès, C. (2015). Trophic dynamics of  
548 scleractinian corals: stable isotope evidence. *Journal of Experimental Biology*, 218(8),  
549 1223-1234.

550 Tremblay, P., Gori, A., Maguer, J. F., Hoogenboom, M., & Ferrier-Pagès, C. (2016).  
551 Heterotrophy promotes the re-establishment of photosynthate translocation in a symbiotic  
552 coral after heat stress. *Scientific reports*, 6, 38112.

553 Tremblay, P., Grover, R., Maguer, J. F., Hoogenboom, M., & Ferrier-Pagès, C. (2014).  
554 Carbon translocation from symbiont to host depends on irradiance and food availability in  
555 the tropical coral *Stylophora pistillata*. *Coral Reefs*, 33(1), 1-13.

556 Tremblay, P., Grover, R., Maguer, J. F., Legendre, L., & Ferrier-Pagès, C. (2012).  
557 Autotrophic carbon budget in coral tissue: a new <sup>13</sup>C-based model of photosynthate  
558 translocation. *Journal of Experimental Biology*, 215(8), 1384-1393.

559 Twining, B. S., & Baines, S. B. (2013). The trace metal composition of marine  
560 phytoplankton. *Annual Review of Marine Science*, 5, 191-215.

561 Usher, K. M., Bergman, B., & Raven, J. A. (2007). Exploring cyanobacterial mutualisms.  
562 *Annual review of ecology, evolution, and systematics*, 255-273.



563 Venn, A. A., Loram, J. E., & Douglas, A. E. (2008). Photosynthetic symbioses in animals.  
564 *Journal of Experimental Botany*, 59(5), 1069-1080.

565 Weis, V. M. (2008). Cellular mechanisms of Cnidarian bleaching: stress causes the collapse  
566 of symbiosis. *Journal of Experimental Biology*, 211(19), 3059-3066.

567 Yellowlees, D., Rees, T. A. V., & Leggat, W. (2008). Metabolic interactions between algal  
568 symbionts and invertebrate hosts. *Plant, cell & environment*, 31(5), 679-694.

569 Zhang, H., Zhuang, Y., Gill, J., & Lin, S. (2013). Proof that dinoflagellate spliced leader  
570 (DinoSL) is a useful hook for fishing dinoflagellate transcripts from mixed microbial  
571 samples: *Symbiodinium kawagutii* as a case study. *Protist*, 164(4), 510-527.

572 Zhu, J. K. (2001). Cell signaling under salt, water and cold stresses. *Current Opinion in Plant*  
573 *Biology*, 4(5), 401-40.

574  
575

576 Figure and Table captions:

577 Figure 1: Principal Component Analysis (PCA) taking into account all data (micronutrient  
578 concentrations in symbionts and host tissue, as well as the isotopic signature of zinc and  
579 copper in each compartments, n = 5 samples for each condition) at 25°C (normal growth  
580 temperature) and 30°C (stress)

581

582 Figure 2: Isotopic signature of copper (d65Cu) and zinc (d66Zn) in (a) symbionts and (b) host  
583 tissue of colonies maintained fed and unfed at 25°C or 30°C; (c) Symbiont density (106  
584 cell/cm<sup>2</sup>) (data are mean and standard deviation of 5 samples per experimental conditions)

585

586 Figure 3: Relationship between the d65Cu and d66Zn values, or between the concentration  
587 (lg/g) in Cu and Zn, Mg and Zn, B and Cu, Ba and Ca, Zn and Ca (n = 5 samples for each  
588 experimental condition). Open circles and squares represent unfed symbionts and host tissue

589 at 25°C (blue) or 30°C (red) respectively. Filled circles and squares represent fed symbionts  
590 and host tissue at 25°C (blue) or 30°C (red) respectively. The arrow indicates the direction of  
591 the distillation process during bleaching

592

593 Figure 4: Heterotrophic supply of micronutrients within the coraldinoflagellate association.  
594 Zooplankton predation increases the amount of Mg, Mn and Fe in symbionts. These metals  
595 are involved in photosynthesis processes, in nitrate reduction and in the structure of  
596 antioxidant enzymes. Prey digestion preferentially releases light copper isotope (i.e.  $^{63}\text{Cu}$ )  
597 and inversely heavy zinc isotope ( $^{66}\text{Zn}$ ), increasing the  $\delta^{65}\text{Cu}$  signature and decreasing the  
598  $\delta^{66}\text{Zn}$  signature of coral tissue. Blue arrows: positive effect

599

600 Figure 5: Schematic diagram summarizing the effect of thermal stress on micronutrient  
601 concentrations in unfed (a) and fed (b) corals. Thermal stress (1) increases ROS (reactive  
602 oxygen species) in coral tissue (2), and induces the disruption of Ca, Sr, Mg and B  
603 homeostasis (3). In unfed corals (a), micronutrient concentrations and antioxidant enzymes  
604 are not produced in sufficient amount to significantly reduce ROS (4). Photosynthesis is  
605 impaired and symbionts are expelled (bleaching). In fed corals (b), feeding increases the  
606 amount of micronutrients in host tissue and symbionts. Antioxidant enzymes are produced in  
607 sufficient amount to significantly reduce ROS (4). Photosynthesis is not impaired and  
608 symbionts are not expelled (no bleaching). Red arrows: negative effect, green arrows:  
609 positive effect

610

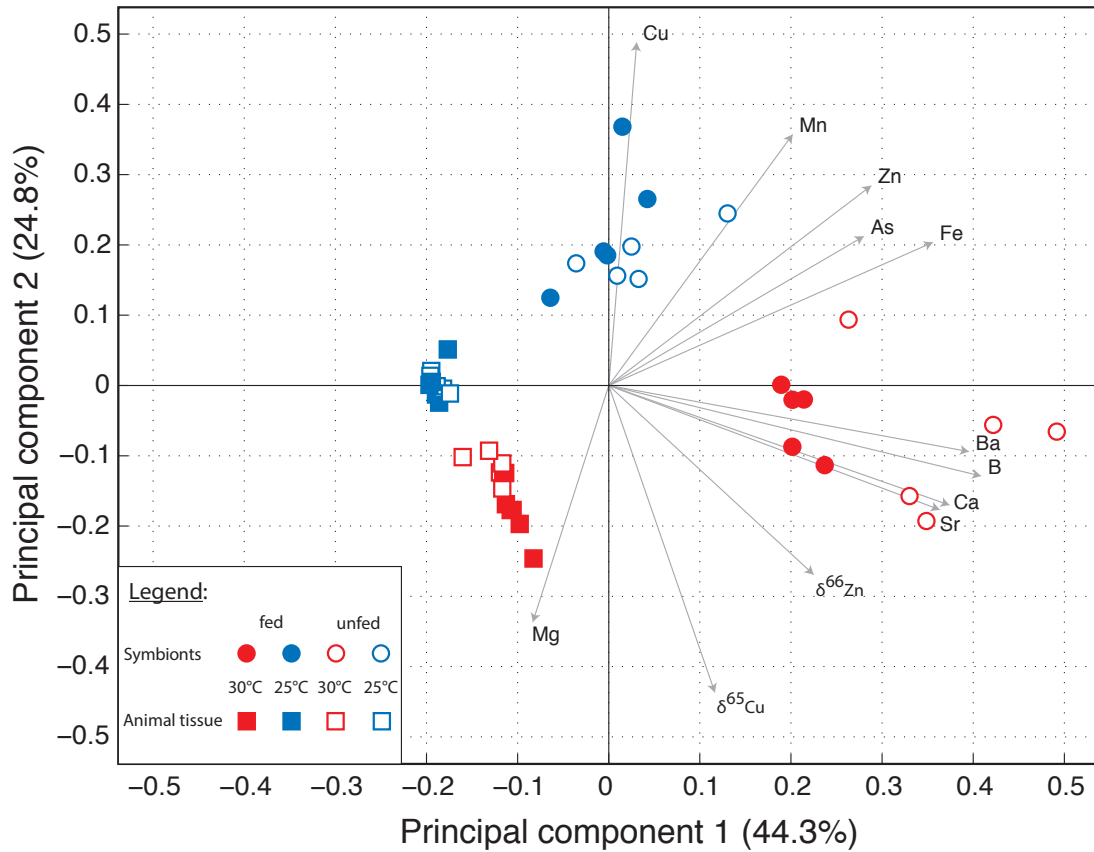
611 Table 1: Micronutrient concentrations (lg/g dry weight) in symbionts and host tissue of fed  
612 and unfed *S. pistillata* maintained under normal (25°C) and thermal stress (30°C) conditions

613

614 Table 2: Results of the two factors ANOVA testing the effects of temperature and feeding on  
 615 the nutrient concentrations and isotopic signatures

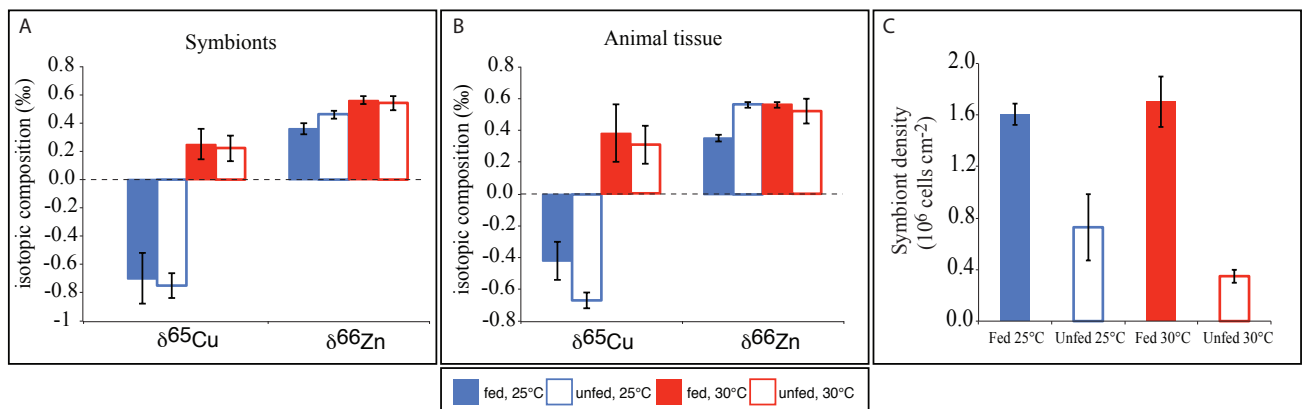
616  
 617  
 618

Figure 1



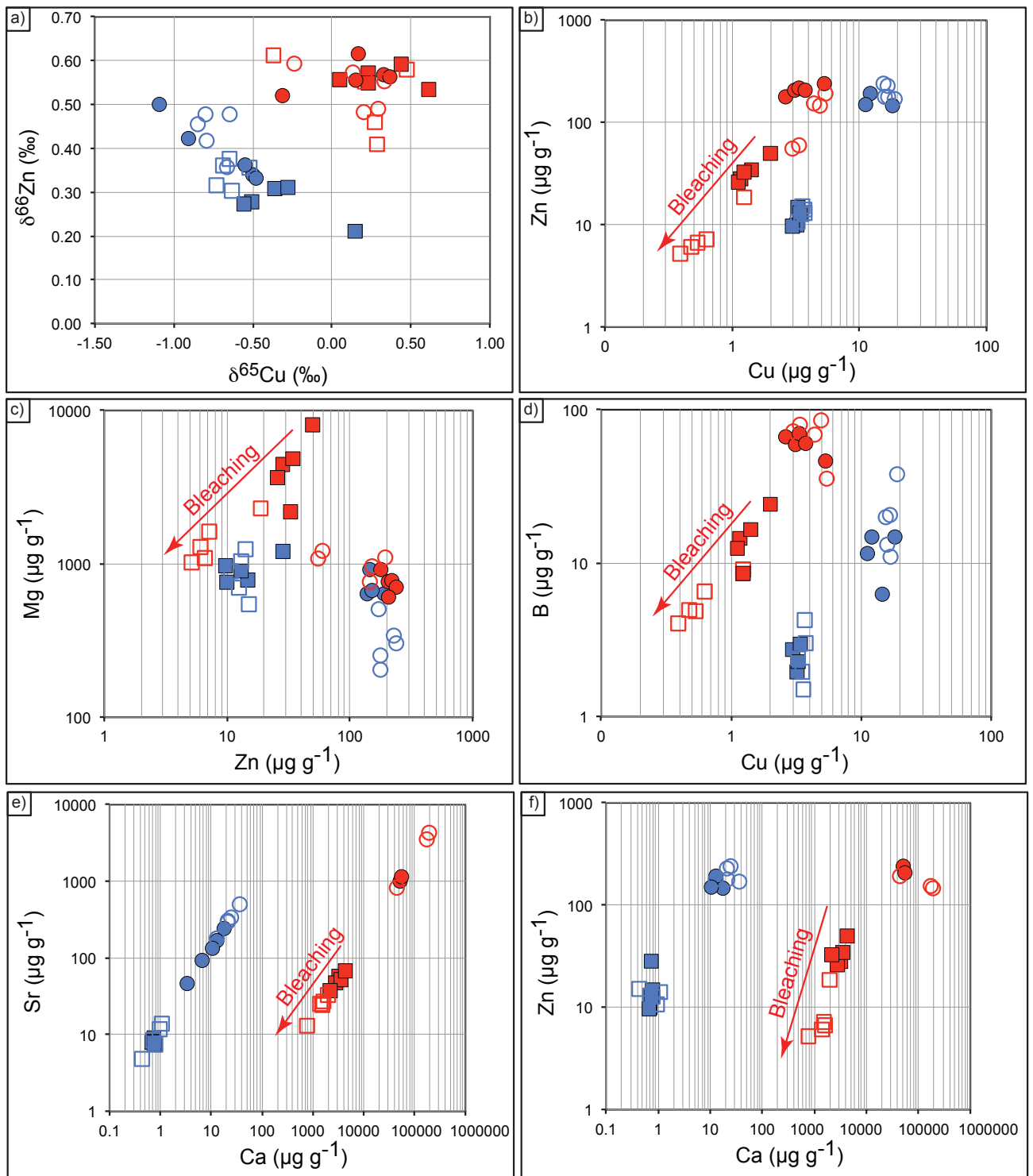
619  
 620  
 621  
 622  
 623

Figure 2



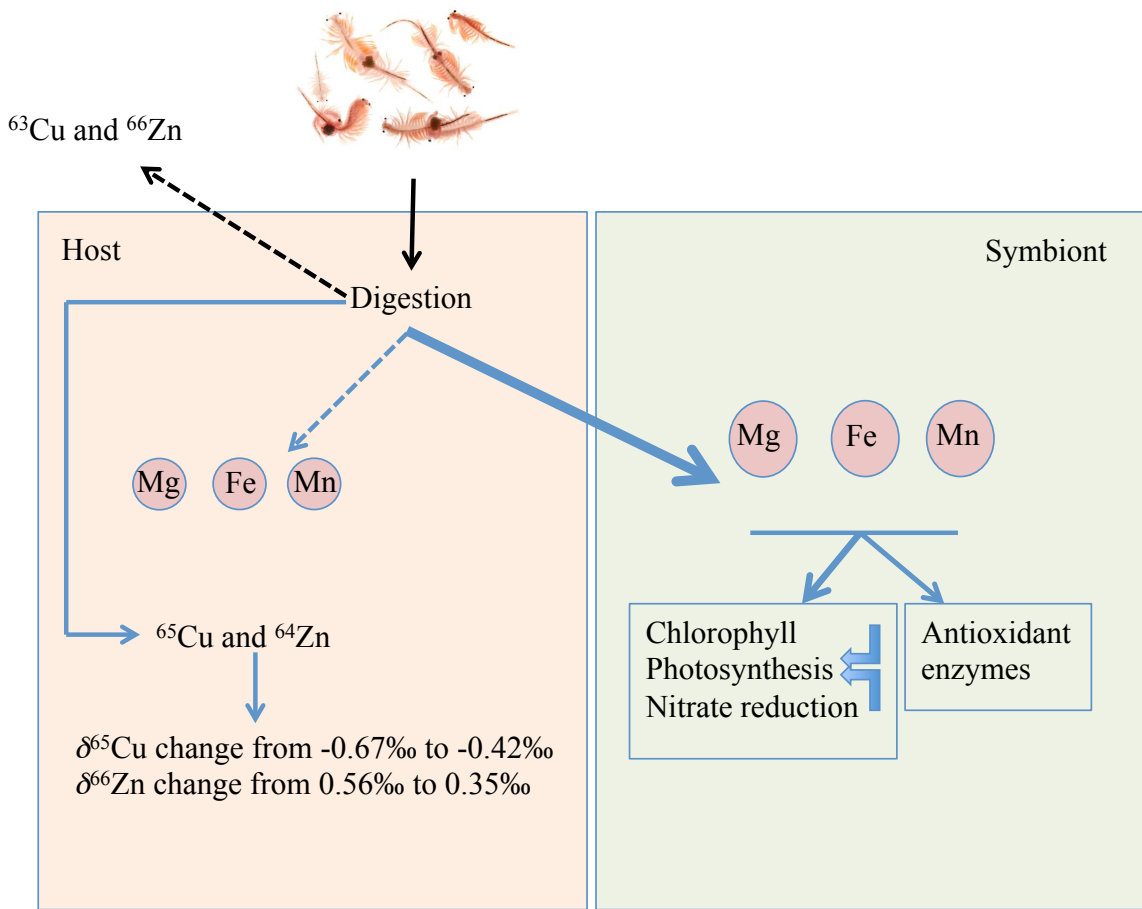
624  
 625  
 626  
 627

Figure 3



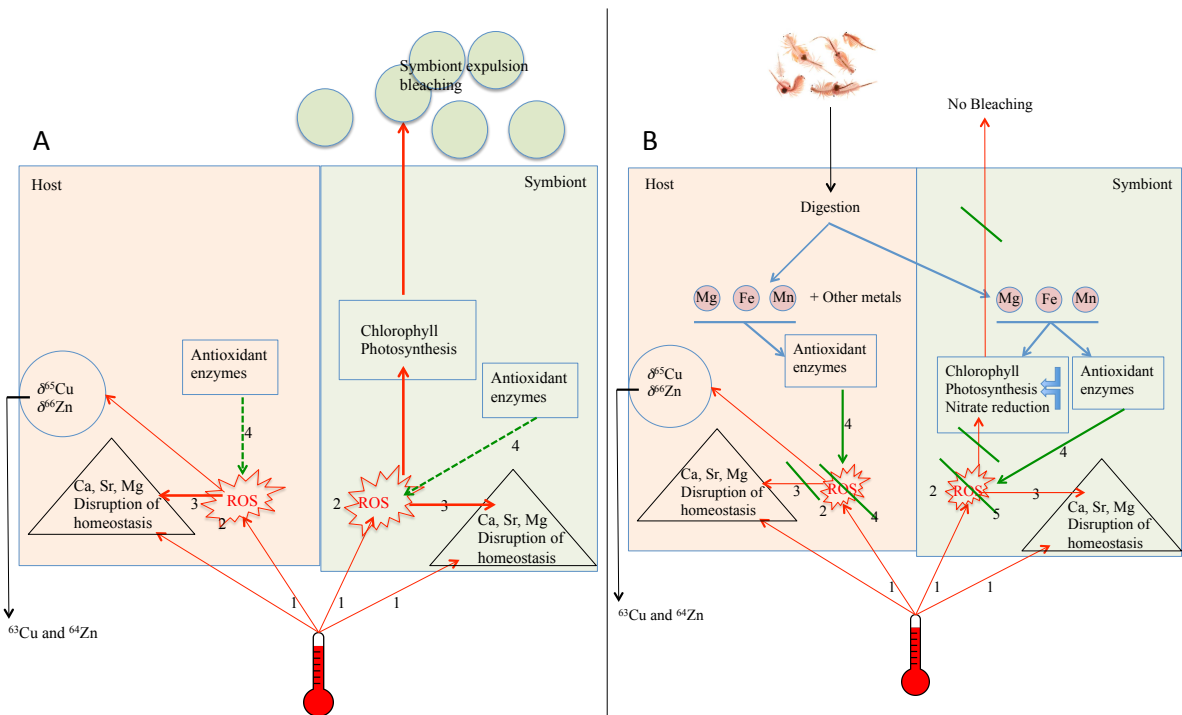
629  
 630  
 631  
 632  
 633  
 634  
 635  
 636  
 637

Figure 4



639  
640  
641  
642

Figure 5



643

644  
645

Table 1

		Higher concentrations in fed symbionts at 25°C			Lower concentrations in fed symbionts at 25°C			Ba	Ca	B	Cu	$\delta^{65}\text{Cu}$ (‰)	$\delta^{66}\text{Zn}$ (‰)
		Mn	Fe	Mg	Zn	Sr	As						
<b>Symbionts 25°C</b>	Fed	6.12*	81.73	659.15	156.61*	160.35*	4.48	0.59*	12.02*	12.86*	14.02*	-0.70*	0.36*
	SD	1.22	13.89	168.28	23.70	64.89	0.86	0.17	4.72	2.27	3.13	0.18	0.04
<b>Symbionts 25°C</b>	Unfed	0.22*	45.83*	275.15*	198.14*	358.77*	10.77	1.22*	23.39*	16.24*	16.76*	-0.75*	0.46
	SD	0.25	4.89	58.82	31.84	94.19	4.07	0.61	8.55	4.79	1.38	0.09	0.03
<b>Symbionts 30°C</b>	Fed	1.19*	83.61	810.45	209.40*	1992*	5.99	2.98*	96242*	60.01*	3.56*	0.25*	0.56*
	SD	0.33	35.15	132.33	20.13	840.41	1.17	1.18	73835	8.28	0.93	0.11	0.03
<b>Symbionts 30°C</b>	Unfed	2.32*	100.84*	864.49*	111.33*	3984*	6.48	4.89*	116904*	59.53*	3.57*	0.22*	0.54
	SD	1.52	57.38	360.29	72.34	1975	3.91	2.16	65108	25.66	1.40	0.09	0.05
<b>Host 25°C</b>	Fed	0.07*	4.22*	924.45*	11.87*	8.02*	1.83*	0.04	0.73*	3.02*	6.59	-0.42*	0.35*
	SD	0.07	0.74	178.86	2.46	0.67	0.28	0.01	0.05	1.25	7.52	0.12	0.02
<b>Host 25°C</b>	Unfed	0.04	3.63	881.99	13.14*	9.24*	1.74*	0.09	0.80*	2.62*	3.55*	-0.67*	0.56
	SD	0.08	0.44	273.63	1.68	3.59	0.27	0.10	0.25	1.07	0.19	0.05	0.02
<b>Host 30°C</b>	Fed	0.35*	11.11*	5670*	31.24*	46.62*	3.32*	0.19	3581*	16.63*	1.36	0.38*	0.56*
	SD	0.10	2.44	2002	3.37	8.49	1.36	0.18	583.86	4.53	0.30	0.18	0.02
<b>Host 30°C</b>	Unfed	0.10	4.45	1360	6.28*	27.06*	3.21*	0.04	1393*	5.84*	0.63*	0.31*	0.52
	SD	0.03	2.06	461.09	0.74	3.51	1.29	0.01	446.35	1.79	0.31	0.12	0.08

646  
647  
648  
649  
650  
651  
652  
653  
654  
655  
656  
657  
658  
659  
660  
661  
662  
663  
664  
665  
666

Table 1: Metal concentrations ( $\mu\text{g g}^{-1}$  dry weight) in symbionts and host tissue of fed and unfed *S. pistillata* maintained under normal (25°C) and thermal stress (30°C) conditions. Data are mean and standard deviation (SD) of 5 samples per condition; \* represents significant differences in metal concentrations between the two temperature conditions for both symbionts and host under fed or unfed conditions.

Table 2

	Symbionts			Tissue		
	df	<i>p</i>	f	df	<i>p</i>	f
<b>Manganese (Mn)</b>						
Feeding	1	<b>0.0010</b>	17.27	1	<b>0.0010</b>	16.04
Temperature	1	<b>0.0273</b>	6.07	1	<b>0.0002</b>	22.89
Feeding × Temperature	1	<b>&lt; 0.001</b>	61.84	1	<b>0.0075</b>	9.36
Error	14					
<b>Iron (Fe)</b>						
Feeding	1	<b>0.0467</b>	4.65	1	<b>0.0004</b>	20
Temperature	1	<b>0.0004</b>	19.61	1	<b>0.0003</b>	21.75
Feeding × Temperature	1	<b>&lt; 0.0001</b>	65.32	1	<b>0.0044</b>	10.95
Error	16			16		
<b>Magnesium (Mg)</b>						
Feeding	1	0.3671	0.86	1	<b>0.0014</b>	14.84
Temperature	1	<b>&lt; 0.0001</b>	48	1	<b>&lt; 0.0001</b>	43.72
Feeding × Temperature	1	<b>&lt; 0.0001</b>	28.43	1	<b>0.0039</b>	11.38
Error	16			16		
<b>Zinc (Zn)</b>						
Feeding	1	0.0419	4.89	1	<b>&lt; 0.0001</b>	45.67
Temperature	1	0.2934	1.18	1	0.4327	0.64
Feeding × Temperature	1	<b>&lt; 0.0001</b>	30.4	1	<b>&lt; 0.0001</b>	38.65
Error	16			16		
<b>Strontium (Sr)</b>						
Feeding	1	<b>0.0105</b>	8.39	1	<b>0.0005</b>	18.89
Temperature	1	<b>&lt; 0.0001</b>	90.03	1	<b>&lt; 0.0001</b>	119.91
Feeding × Temperature	1	0.3487	0.93	1	<b>0.0002</b>	22.85
Error	16			16		
<b>Arsenic (As)</b>						
Feeding	1	<b>0.0048</b>	10.7	1	0.5212	0.43
Temperature	1	0.6682	0.17	1	<b>0.0008</b>	18.83
Feeding × Temperature	1	0.1279	2.58	1	0.6728	0.19
Error	16			16		
<b>Barium (Ba)</b>						
Feeding	1	<b>0.0021</b>	13.49	1	0.5284	0.18
Temperature	1	<b>&lt; 0.0001</b>	52.96	1	0.2393	0.34
Feeding × Temperature	1	<b>0.0438</b>	4.79	1	<b>0.0357</b>	5.66
Error	16			16		
<b>Calcium (Ca)</b>						
Feeding	1	<b>0.0223</b>	7.02	1	<b>0.0075</b>	8.75
Temperature	1	<b>&lt; 0.0001</b>	744.93	1	<b>&lt; 0.0001</b>	650.5
Feeding × Temperature	1	0.82	0.05	1	<b>0.0035</b>	12.11
Error	11			16		

<b>Boron (B)</b>						
Feeding	1	<b>0.0052</b>	10.43	1	<b>0.0042</b>	11.15
Temperature	1	<b>&lt; 0.0001</b>	132.15	1	<b>&lt; 0.0001</b>	56.67
Feeding × Temperature	1	<b>0.0294</b>	5.71	1	<b>0.0275</b>	5.89
Error	16			16		
<b>Copper (Cu)</b>						
Feeding	1	<b>0.0336</b>	5.4	1	0.2796	1.25
Temperature	1	<b>&lt; 0.0001</b>	222.68	1	<b>0.0286</b>	5.78
Feeding × Temperature	1	0.141	2.4	1	0.5027	0.47
Error	16			16		
<b><math>\delta^{65}\text{Cu}</math></b>						
Feeding	1	0.8399	0.04	1	<b>0.0455</b>	4.7
Temperature	1	<b>&lt; 0.0001</b>	72.23	1	<b>&lt; 0.0001</b>	44.26
Feeding × Temperature	1	0.8398	0.04	1	0.3745	0.83
Error	16			16		
<b><math>\delta^{66}\text{Zn}</math></b>						
Feeding	1	0.6455	0.22	1	0.5186	0.44
Temperature	1	<b>&lt; 0.0001</b>	33.11	1	<b>&lt; 0.0001</b>	103.31
Feeding × Temperature	1	0.1159	2.76	1	<b>0.0331</b>	5.44
Error	16			16		

669